A Viscous Compressible Model for Stress Generation/Relaxation in SiO_2

Mitra Navi and Scott T. Dunham

Electrical, Computer and Systems Engineering Department
Boston University, Boston, MA 02215.

Abstract

In this work, a model has been developed and characterized to account for the mechanical behavior of silicon dioxide and its effect on oxidation kinetics. Conservation of mass, momentum balance, and the transport equation along with appropriate boundary conditions have been formulated. The material law used for the oxide is that of a compressible viscous material applied via mass and momentum balance (Navier-Stokes equation). The oxidation is modeled by a steady-state diffusion of oxidants, with reaction at the Si/SiO_2 interface. Due to the volume difference, the newly created oxide is assumed to be highly compressed, relaxing as oxidation (or annealing) proceeds. Thus, thermal history effects which occur even in planar oxides can be accounted for. Mechanical behavior of the oxide is characterized based on stress relaxation data. The model is then matched to both two-step and single-step oxidation kinetics, extracting stress-dependent diffusivity and solubility parameters.

1 Introduction

Thermal oxidation of silicon is an essential step in VLSI technology. Modeling the process is necessary for predicting the oxide shape and thickness. Due to the volume expansion during oxidation, large stresses exist in the oxide [1]. Measurements of oxide refractive index show that the stress increases for oxides grown at lower temperatures [2, 3], in agreement with the observation that annealing of oxides grown at low temperature causes the films to swell [4, 5]. The reduced oxide thickness grown on silicon corners indicates that stress can reduce the growth coefficients [6] and experiments indicate that the diffusivity as well as the solubility of oxidizing species are likely to be influenced by this stress [7]. Fargeix *et al.* [8] reported that local compressive stress exists in the SiO_2 which is at its maximum at the Si-SiO_2 interface and decreases monotonically towards the free surface of the oxide. They suggested that molecular diffusivity in such a stressed film is therefore lower than the same film when unstressed.

Oxide layers with various stress levels can be generated by varying the growth temperatures. Thus, the dependence of growth rate parameters on stress in the oxide can be studied by comparing the additional thickness of the oxide grown underneath differently stressed layers. The two-step oxidation experiments such as those performed by Landsberger *et al.* [9] can therefore be used to understand history effects in thermal oxide and to quantify the dependence of growth parameters on generated stress during oxidation.

Isolation technologies such as local oxidation of silicon (LOCOS), buried oxide (BOX) and deep trench have been modeled by a number of workers [10, 11]. In many of these analyses, fullly viscoelastic models have been developed to predict the oxide shape by including the dependence of oxidation parameters on stress. However, models which consider stress-dependent oxidation in 2 and 3D structures, generally ignore the higher density of oxide produced at lower temperatures even in planar structures [7, 10, 11, 12]. Thus the baseline for "stress free" diffusivity and solubility used in these models are actually the values at the stresses typical of oxides grown at those temperatures, which relaxation and two-step oxidation experiments [4, 13, 14] clearly reveal as very different from the true "stress free" values.

In this work, we develop a model for stress generation/relaxation and its effect on oxidation kinetics, which includes the initial formation of a high density oxide. Analysis of oxide relaxation experiments are used to extract the mechanical characteristics of SiO_2 films. The model is then applied to one [15] and two-step oxidation kinetics [9] and stress-dependent oxidant diffusivity and solubility are extracted.

2 Modeling

To be able to accurately predict oxide thickness as a function of time, one must first establish the mechanical models for oxidation. Depending on temperature, one can expect the oxide to behave as a solid or fluid. A number of models have been proposed to describe the behavior of oxide [16, 17, 18]. In this work, a compressible viscous model, which represents a distributed (spatially varying) version of the model used by Rafferty *et al.* [16] is proposed to account for the behavior of SiO_2.

To construct the model, we first express the principle of conservation of mass in the oxide as:

$$\frac{\partial \rho}{\partial t} + \frac{\partial (\rho V)}{\partial x} = 0, \tag{1}$$

where ρ is the mass density of the material and V is the velocity. Next, the momentum balance for steady flow is described by the Navier-Stokes equation as:

$$\rho(\frac{\partial V}{\partial t} + V\frac{\partial V}{\partial x}) = \frac{\partial \sigma}{\partial x}, \tag{2}$$

where σ denotes the stress. Finally material law, for a compressible viscous material is:

$$\sigma = -P + (\lambda + 2\mu)\,\frac{\partial V}{\partial x}, \tag{3}$$

where P is the pressure, λ is the Lame constant and μ is the viscosity. Furthermore, the pressure P is related to mass density by:

$$P = P_0 + P_1\frac{\rho - \rho_1}{\rho_1}, \tag{4}$$

where P_0 is the atmospheric pressure, P_1 is the Young modulus of SiO_2 [19], and ρ_1 is the equilibrium oxide density ($\sim$ 2.22 gr/cm^3). In this model, the viscosity (μ) is allowed to depend on stress such that [12]:

$$\mu = \mu_0\,\frac{\sigma/\sigma_c}{\sinh(\sigma/\sigma_c)}. \tag{5}$$

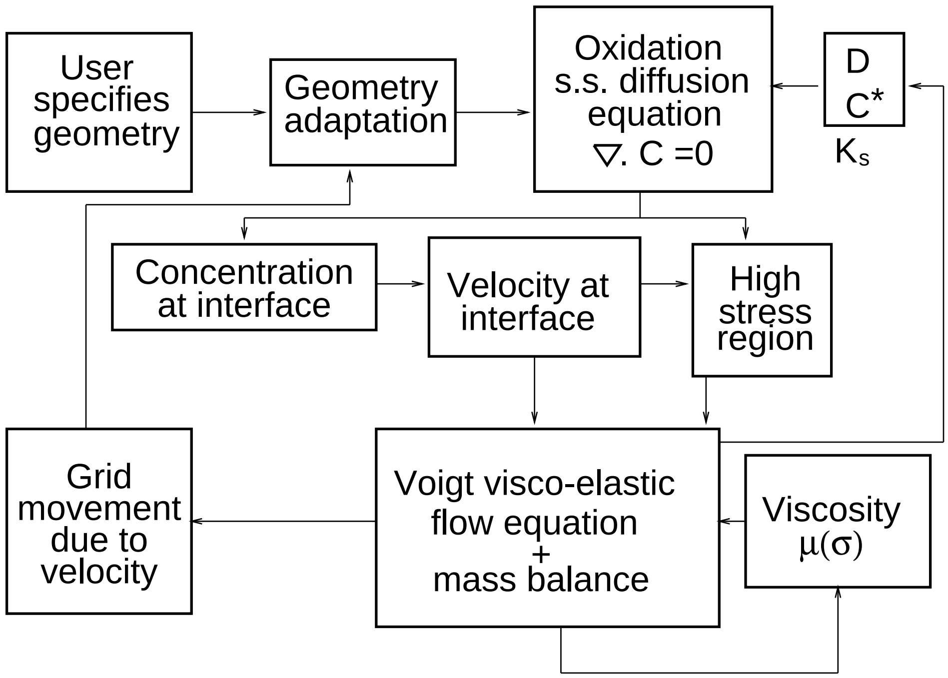

Figure 1: An overview of the 1D finite element solution method

Next, we have to account for the oxidant diffusion through the oxide and reaction at the interface. As mentioned previously, stress generated during oxidation can affect the diffusivity (D) and solubility (C^*) of the oxidant species. The diffusivity and solubility can be written in the form [7]:

$$D = D_0 \exp\frac{(-PV_D)}{kT}, \tag{6}$$

$$C^* = C_0^* \exp\frac{(-PV_C)}{kT} \tag{7}$$

where V_D and V_C are the activation volume for diffusion and solubility respectably. For the 1D systems considered in this work, there is no normal stress so the interface reaction rate k_s is fixed. Incorporating the above assumptions, one can represent the transport equation for oxidizing species as:

$$\frac{\partial}{\partial x} DC^* \frac{\partial C/C^*}{\partial x} = 0, \tag{8}$$

where C is the concentration and D is the diffusion constant of the oxidizing species. The above equation is assumed to be in steady state and subject to boundary conditions:

$$DC^* \frac{\partial C/C^*}{\partial x} = k_s C, \tag{9}$$

at the Si/SiO_2 interface ($x = 0$) and

$$DC^* \frac{\partial C/C^*}{\partial x} = h(C - C^*), \tag{10}$$

at the SiO_2/gas interface ($x = x_o$) where h is the gas-phase transport coefficient. The solution to Eq. 8 provides the boundary conditions for the velocity. However, instead of generating a large volume of unstressed oxide, as is most commonly done [15, 20], we assume

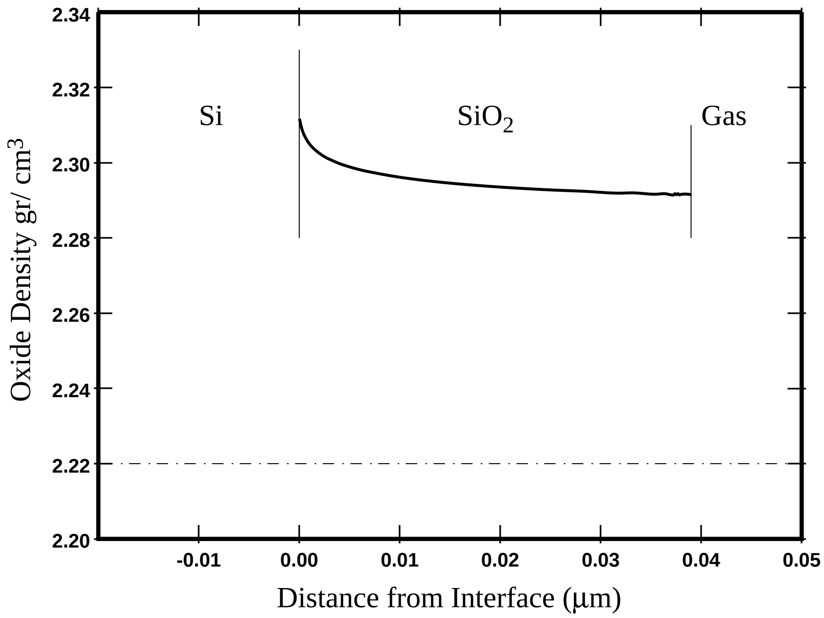

Figure 2: Simulated density distribution for an oxide film grown at 800°C in dry O_2 on $\langle 111\rangle$ silicon. The equilibrium oxide density is also displayed as reference.

that a region of high stress is created with the same volume as the silicon consumed [21] and density

$$\rho = m_{ox} C_{si}, \tag{11}$$

where m_{ox} is the molecular mass of the oxide and C_{si} is the atom concentration of silicon (as opposed to SiO_2). This high density region is relaxed by solving the coupled partial differential equation of mass and momentum balance, which also contributes to the growth of the oxide.

It can be noted that the equations for mass (Eq. 1) and momentum balance (Eq. 2) are two coupled nonlinear partial differential equations. These equations cannot easily be solved by analytical techniques. Therefore numerical techniques are essential. A one dimensional finite element discretization of the above model has been implemented. Figure 1 shows the numerical computation flow chart for a typical time step.

3 Results and Discussion

Figure 2 shows the result of the above model for a 500 min oxidation at 800°C. The high stress generated at the interface $\rho = m_{ox} C_{si}$ (~ 4.99 gr/cm^3) relaxes almost immediately to a value of about 2.31 gr/cm^3 at 800°C. This value is calculated from the amount of relaxation in the time it takes to grow half a monolayer of oxide. This rapid relaxation is due to the strongly nonlinear behavior of viscosity at high stresses. For stress in the oxide greater than the critical stress σ_c, the viscosity reduces, causing the oxide to flow much more readily. The non-uniformity of the density profile in the oxide is due to the fact that relaxation occurs for

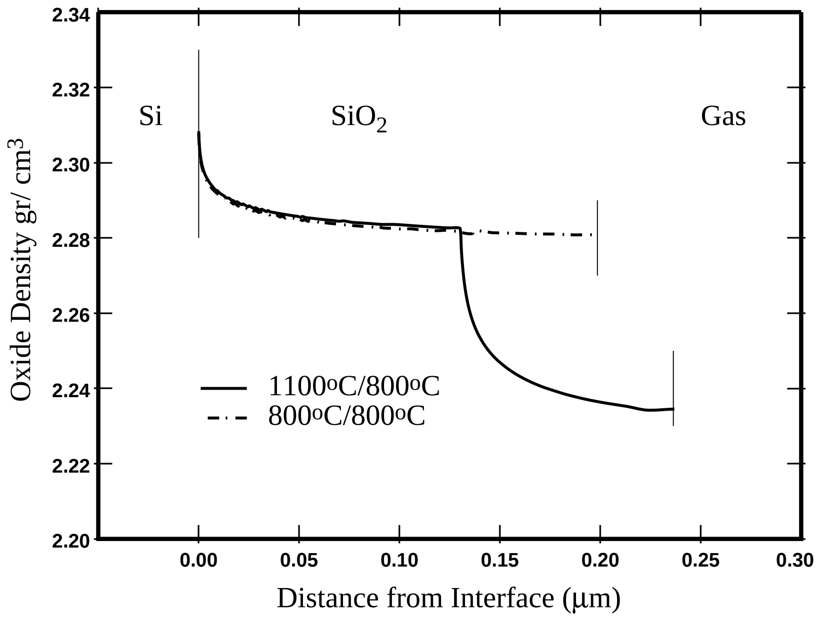

Figure 3: Simulated density distribution for oxides grown at 1100 and 800°C to a thickness of 1070Å and subsequently reoxidized at 800°C for 65h.

the already formed SiO_2, as this oxide is continuously exposed to the high temperature. This is in agreement with the *in situ* SiO_2 stress measurements as a function of oxide thickness reported by Kobeda *et al.* [1].

Using viscosity in unstressed SiO_2 (μ_0) from data on bulk silica [22], the model was matched to oxide relaxation data of Landsberger *et al.* [9] to extract the parameter σ_c. The relaxation experiments were as follows. Dry oxide films grown on lightly doped p-type Si $\langle 111 \rangle$ wafers at 800°C were annealed in inert ambients. The annealing process caused the oxide to swell by $\sim$3% of its as-grown thickness. Figure 4 shows the fit of the model to this data and Table 1 shows the extracted σ_c for various temperatures. Also shown are the values of σ_c extracted by Rafferty *et al.* [16]. The difference can be attributed primarily to the fact that Rafferty used not only σ_c but also the value of viscosity for unstressed oxides as fitting parameters finding a lower bulk viscosity. In addition, the model used in this work considers the variation of stress within the film, rather than assuming a homogeneous film as in the model used by Rafferty *et al.* [16]. This allows the application of the same model to oxidation kinetics through the dependence of diffusivity and solubility on local excess density in the SiO_2.

Once the mechanical parameters were established, the model was further matched to two-step oxidation experiments [9] and standard one-step oxidation kinetics [23], optimizing the stress dependent diffusivity and solubility parameters. The solubility of O_2 at 1 atm in unstressed oxide is taken from permeation experiments for vitreous silica ($C_0^* = 1.1\times10^{16}$ $\exp(0.17/kT)$ cm^{-3} [24]) and the activation volume for diffusion and solubility are assumed equal ($V_C = V_D$). In two-step oxidation experiments [9], the amount of oxide grown in the second step depends greatly on the growth temperature used in the first step. This is

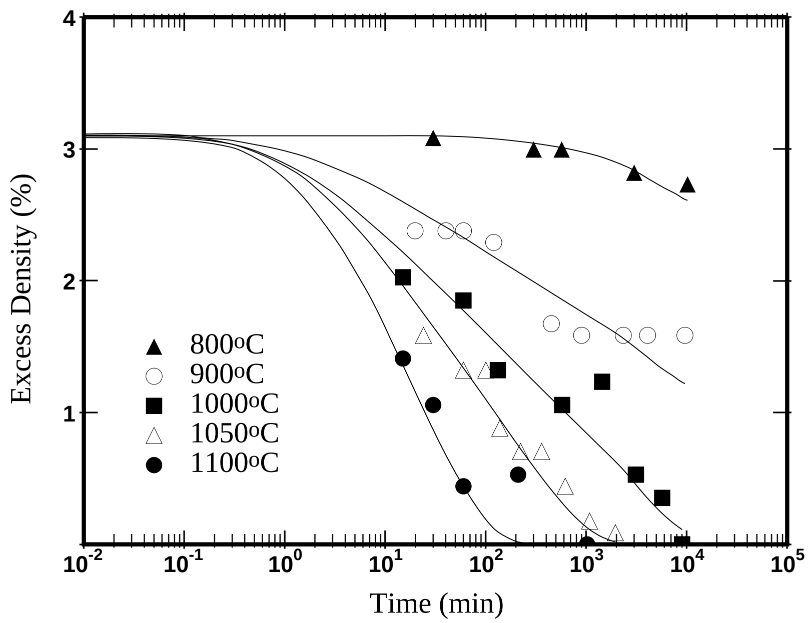

Figure 4: Excess oxide density versus annealing time over a range of temperatures. Data from Landsberger *et al.* [4]. Note that the model predicts the original excess density as well as the relaxation kinetics.

accounted for by the dependence of the diffusivity and solubility on the stress distribution in the oxide. Figure 3 shows the simulated density distributions in oxides grown to a thickness of 1070Å at either 1100 or 800°C and then oxidized at 800°C for 65 hours. As is seen experimentally [9], the films which are grown with an initial higher temperature oxidation experience an enhanced oxidation rate for the second step. The reasons for this behavior are illustrated in Figure 3, where the lower density of oxide grown at higher temperature leads to higher oxidant solubility and diffusivity.

The model accounts for both two-step and one-step oxidation kinetics data over a temperature range of 800−1180°C as illustrated in Figure 5. The three curves which start with an initial oxide thickness of 1070Å correspond to the two-step oxidation experiments [9]. Note that thermal history effects are due to the greater oxide relaxation for film grown at higher temperatures. The activation volumes ($V_D = V_C$) and the stress-free values for the diffusivity and interface reaction rate are fitted to both one-step as well as two-step oxidation kinetics data. Table 2 provides a summary of the parameters used.

Figures 6 and 7 show the extracted values of unstressed diffusivity (D_0) and interface reaction rate (k_s) for dry oxidation of ⟨111⟩ Si. Also plotted are the values of D and k_s calculated from the results of Massoud *et al.* [15] and Landsberger *et al.* [9] using $C_0^* = 1.1\times10^{16}\exp(0.17/kT)$ cm^{-3} [24]. It can be noted that the optimized values of the diffusivity and interface reaction rate are larger than values reported by previously [15, 20]. This difference is attributed to the fact that effective values extracted for these parameters are generally reduced due to the presence of stress in the oxide, while values for these parameters extracted from our model reflect the diffusivity and reaction rate for an unstressed oxide.

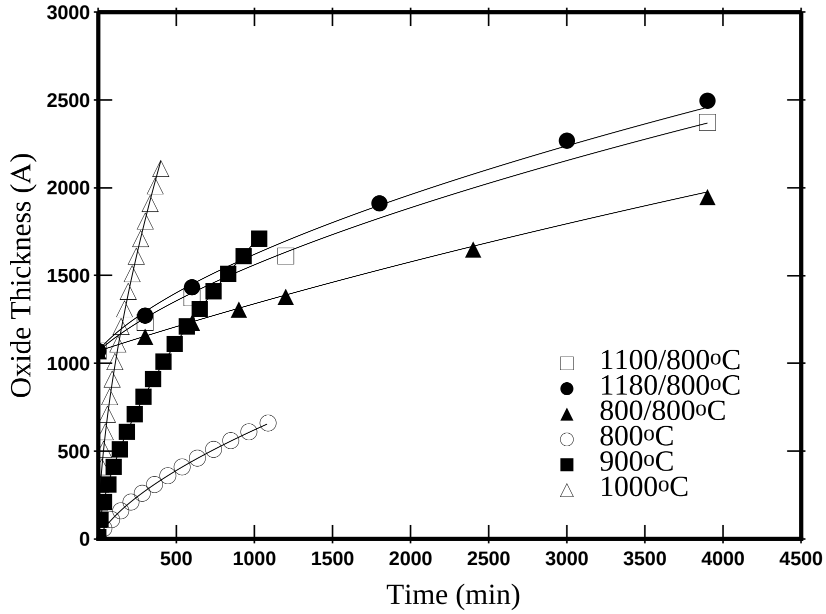

Figure 5: Comparison of model simulation to two-step [9] and one-step oxidation kinetics data [23].

At higher temperatures, bulk density approaches the equilibrium density and effective parameters might be expected to approach the values in unstressed oxide. Figure 6 depicts this trend: At higher temperatures, the diffusivity from above model approaches reported effective diffusivities. This is further supported by the fact that the activation energy for D_0 (0.96 eV) is similar to that reported for high temperature oxidation [14, 20]. The diffusivity values reported in this work are very similar to the values reported by Landsberger *et al.* [9] for 1180°C oxides that were reoxidized at lower temperatures (see Figure 6) consistence with the fact that oxides grown at such a high temperature are nearly fully relaxed.

In contrast to diffusivity the extracted reaction rates do not approach the reported effective values even at high temperatures (see Figure 7). There are two factors that account for this behavior. The first factor is the effect of stress at the interface on solubility of oxidizing species. Although the stress at the interface reduces at high temperatures, its temperature dependence is relatively weak due to the nonlinear viscosity. This results in a reduced C^* at the interface even for higher temperatures, which reduces the concentration of oxidizing species at the interface. To be able to account for oxidation kinetics, the reaction rate must then be increased. Secondly the region of maximum stress near the interface reduces the diffusivity considerably. Again this reduces the availability of oxidizing species, requiring a larger reaction rate.

Figure 8 shows a comparison between thin oxide kinetics of Massoud [23] and the model of stress-dependent oxidation developed in this work. Although the model was developed primarily to account for relaxation and two-step oxidation, it also does a very good job predicting behavior in the thin oxide regime. The explanation for the initially rapid oxidation predicted by the model is that for thicker oxides, a compressed region near the interface is

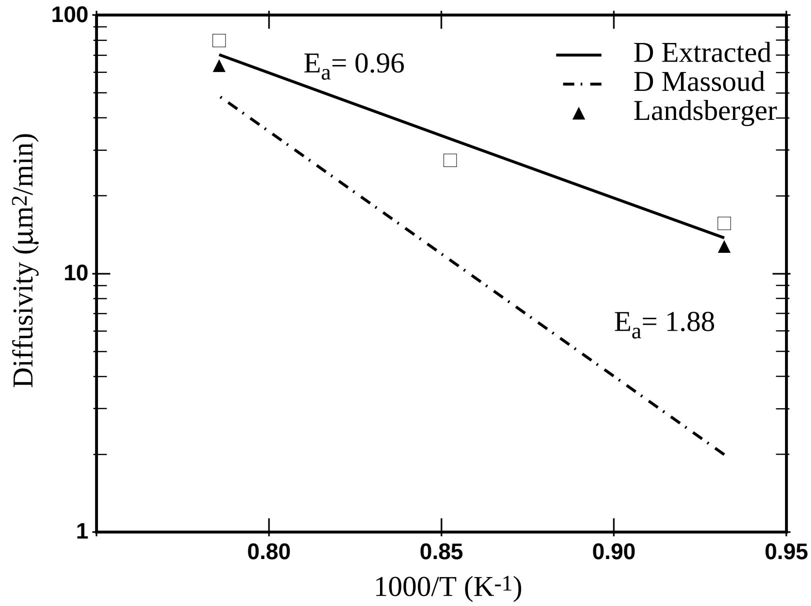

Figure 6: Extracted values of O_2 diffusivity in unstressed SiO_2 as function of temperature and comparison to values based on works by Massoud *et al.* [15] and Landsberger *et al.* [9].

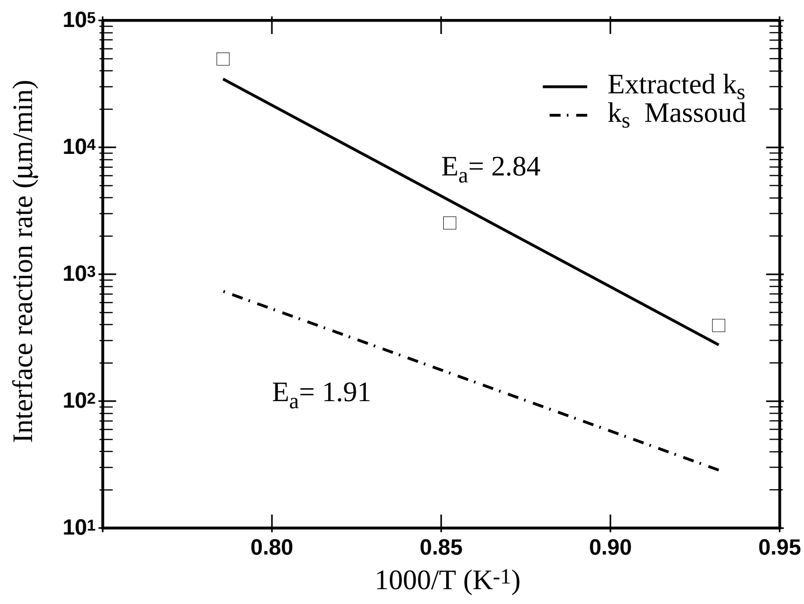

Figure 7: Extracted interface reaction rate values for O_2 as function of temperature for oxidation of ⟨111⟩ silicon and comparison to values calculated from model without stress dependent oxidation [15].

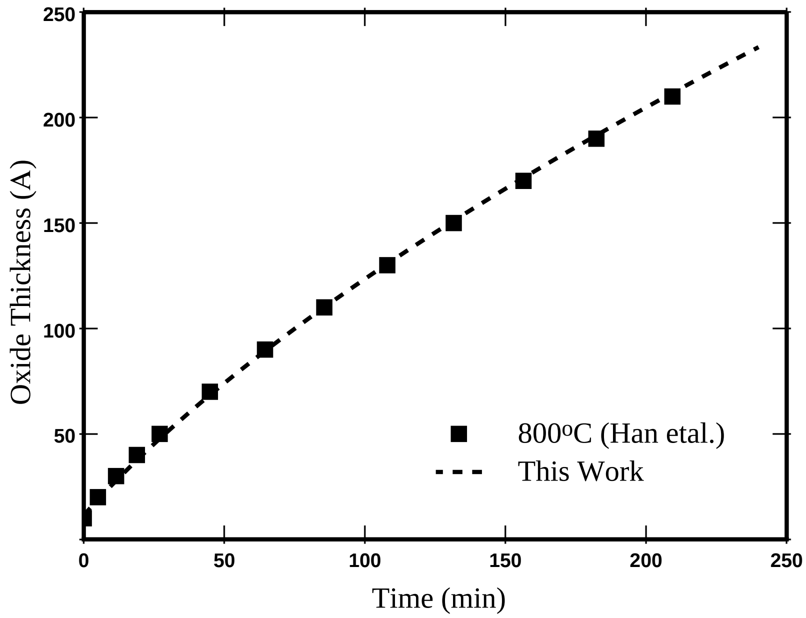

Figure 8: Comparison of model to oxidation kinetics in the thin regime from two-stream model of Han [23] fitted to data of Massoud [15].

established, with a thickness that varies only slowly as the film grows. For moderate oxide thicknesses, it is the combination of the slower diffusion through this interface layer and the interface reaction which limits the growth rate. For very thin films, this layer has not yet been fully established and thus the initial growth rate is higher than the linear growth rate that would be extracted by including only thicker films.

4 Conclusions

A compressible viscous model has been developed to account for the oxidation of silicon. In this model, a highly compressed oxide is created at the Si/SiO_2 interface and is relaxed by solving the equations for mass and momentum balance in the bulk of the oxide. A 1D oxidation code has been developed to solve these equations and mechanical parameters were optimized to relaxation data. The model was further extended to include the stress dependence of oxidation rate parameters. These parameters were fit to oxidation kinetics reported in the literature. A stress-dependent diffusivity (D) and interface reaction rate (k_s) have been extracted for $\langle 111 \rangle$ Si. The model accounts for the oxide relaxation behavior as well as thermal history effects on oxidation kinetics and thin oxide kinetics.

Once the stress dependent viscosity, diffusivity and solubility are characterized based on the 1D analysis used in this work, 2D experiments (e.g. cylindrical oxidation experiments of Kao [7]) can be used to quantify the stress dependent interface reaction rate. The equations described in this work can be easily extended to higher dimensions through the use of full 2 or 3D equations for the mass and momentum balance, the material law and oxidant transport. The primary difference from current 2 or 3D implementation would be the formation of an initial high density oxide at the interface, which allows the use of true "stress free" values as the base-line for oxidation parameters.

5 Acknowledgements

The authors gratefully acknowledge Dr. Norbert Strecker for his assistance with modeling the mechanical system and his helpful discussion in developing the numerical code. This work was supported by SRC grants SJ-530 and BJ-530.

References

[1] E. Kobeda and E. A. Irene. *J. Vac. Sci. Technol.* **7**, 163 (1989).

[2] E. A. Taft. *J. Electrochem. Soc.* **125**, 968 (1978).

[3] A. Szekeres and P. Danesh. *Semicond. Sci. Technol.* **11**, 1225 (1996).

[4] L. M. Landsberger and W. A. Tiller. *Appl. Phys. Lett.* **51**, 1416 (1987).

[5] E. A. Irene, E. Tierney, and J. Angilello. *J. Electrochem. Soc.* **129**, 2594 (1982).

[6] Y. Sakina, T.Ohno, and S. Matsumoto. *Japan. J. Appl. Phys.* **22**, L514 (1983).

[7] D. Kao, J. P. McVittie, W. D. Nix, and K. C. Saraswat. In **IEDM Proc.**, p.388 (1985).

[8] A. Fargeix and G. Ghibaudo. *J. Appl. Phys.* **54**, 7154 (1983).

[9] L. M. Landsberger and W. A. Tiller. *J. Electrochem. Soc.* **137**, 2825 (1990).

[10] Vincent Senez, Dominique Collard, and Bruno Baccus. *J. Appl. Phys.* **76**, 3285 (1994).

[11] S. Cea and M. Law. In **Simulation of Semiconductor Devices and Processes, Austria**, p.139 (1995).

[12] C. S. Rafferty. PhD thesis, Stanford University (Dec. 1989).

[13] N. E. McGruer, R. Singh, J. H. Weiss, and K. Rajikanan. *J. Appl. Phys.* **62**, 3405 (1987).

[14] E. A. Irene. *J. Electrochem. Soc.* **125**, 1708 (1978).

[15] H. Z. Massoud, J. D. Plummer, and E. A. Irene. *J. Electrochem. Soc.* **132**, 1745 (1985).

[16] C. S. Rafferty, L. M. Landsberger, R. W. Dutton, and W. A. Tiller. *Appl. Phys. Lett.* **54**, 151 (1989).

[17] N. Saito, H. Miura, S. Sakata, M. Ikegawa, T. Shimizu, and H. Masuda. In **IEDM Proc.**, p.696 (1989).

[18] K. Schott, A. Seidl, and J. Lorenz. In **Semiconductor Silicon 1990**, p.417–24 (1990).

[19] S. Spinner. *J. Am. Ceramic Soc.* **39**, 113 (1956).

[20] B. E. Deal and A. S. Grove. *J. Electrochem. Soc.* **36**, 3770 (1965).

[21] M. Navi and N. Strecker. In **Meeting of the Electrochemical Society. Miami, Florida**, p.4.3.1–4.3.4 (1994).

[22] G. Hetherington, K. Jack, and J. Kennedy. *Phy. and Chem. of Glasses* **5**, 130 (1964).

[23] C. J. Han and C. R. Helms. *J. Electrochem. Soc.* **134**, 1299 (1987).

[24] F. J. Norton. *Nature* **171**, 701 (1961).

Extracted Critical Stress					
$\sigma_c (10^9$ dynes/cm$^2)$	800°C	900°C	1000°C	1050°C	1100°C
This work	0.94	0.94	1.49	2.17	3.58
Rafferty [16]	0.43	0.43	0.66	0.82	0.88

Table 1: Extracted value of σ_c for various temperatures for this work and from Rafferty *et al.* [16].

Model Parameters			
Parameter Description	Activation Energy	Pre-exponential	Source
Diffusivity of O_2 in Unstressed SiO_2 (D_0)	0.96 (eV)	4.6×10^5 (μm^2/min)	Fitting Parameter
Interface reaction rate in unstressed SiO_2 (k_s)	2.84 (eV)	6×10^{15} (μm/min)	Fitting Parameter
Activation volume ($V_C = V_D$)	–	$13.8 \mathring{A}^3$	Fitting Parameter
Solid solubility of O_2 in unstressed SiO_2 (C^*)	-0.17(eV)	1.1×10^{16} (cm^{-3})	Permeation Experiments [24]
Viscosity of unstressed SiO_2 (μ_0)	-7.045(eV)	3.1×10^{-13} (poise)	Bulk silica [22]
Bulk Modulus of SiO_2 (P_1)	–	4.5×10^{11} (dynes/cm^2)	From Spinner [19]

Table 2: Summary of model parameters used in this work